5th International Conference on Experimental Fluid Mechanics - ICEFM 2018 Munich
Munich, Germany, July 2-4, 2018

Effect of taper on cavitation in a 2D flow channel

Markus Hosbach[1,2*], Tobias Sander[1], Uwe Leuteritz[2], Michael Pfitzner[1]

[1]Bundeswehr University Munich, Germany;
[2]Continental Automotive GmbH, Regensburg, Germany
[*]Corresponding author, Markus Hosbach: markus.hosbach@unibw.de

Abstract

Cavitation erosion plays an important role in the development of new hydraulic components for fuel injection systems. Due to the high pressure level, the corresponding flow speed and limited optical accessibility in real fuel injectors, a test bench consisting of a high pressure generator and a 2D flow channel covered by sapphire windows is used. Calibration fluid ISO 4113 serves as flow medium. A shadowgraph setup is applied for the optical measurements to evaluate the cavitation length and the velocity field. Cavitation length as a function of taper and back pressure as well as the velocity in a converging-diverging flow channel are investigated. It was found that the converging flow channel shows no change in cavitation length when lowering the back pressure. The cavitation length suddenly increases in the parallel and diverging throttle when reaching the cavitation transition point. In the present case temperature has no significant influence on the normalized cavitation length as a function of the normalized cavitation number. For a deeper understanding of the overall flow conditions, first basic velocity measurements of the phase boundary in the diverging part of a converging-diverging flow channel were carried out. No seeding particles are used as cavitation structures serve as tracers for the image evaluation. It was found that the velocity of phase boundary is lower than the velocity derived from the measured mass flow. A change in the shape of velocity profiles when lowering the back pressure was identified. A recirculation flow and eddy formation at the cavitation tip is visible.

1 Introduction

Cavitation can be described as the phase change from liquid to vapor by lowering the static pressure below the saturation pressure. As a consequence of surface tension, the pressure inside the bubble is higher than the pressure in the surrounding liquid and the cavitation bubble grows. If such cavitation bubbles filled with vapor move to areas, where the static pressure exceeds the saturation pressure and collapse close to a solid wall, damage can occur. This erosive wear can take place in high pressure components of gasoline and diesel fuel injection systems like pumps and injectors and can have negative effects on the component durability and consequently on the mixture generation. This in turn can affect the performance and exhaust emissions of modern engines.
Velocity measurements based on shadowgraph-like images in a cavitating flow were investigated in Mauger et al. (2014). The authors found that velocity fluctuations increase with cavitation length. Channel height changed velocity fluctuations whereas liquid temperature had no influence. In super cavitation regime velocity fluctuations strongly increase. Super cavitation is the flow regime beyond the cavitation transition point, where the cavitation length distinctly increases Sou et al. (2007).
In Schmidt et al. (2016) a converging-diverging glass nozzle is used for PIV measurements in water. The inlet pressure is set to about 10 bar. Velocities up to 14 m/s could be measured. Recirculating flows near the wall whose position is related to the cavitation front were found. A periodically oscillating re-entrant motion between the cavity and the wall of a convergent-divergent nozzle in water is found in Sato et al. (2013). Pressure waves caused by collapsing cavities are considered as reason for re-entrant motions, subsequently stated in Hayashi and Sato (2014).
In the present work, the focus lies on the visualization of cavitation and flow conditions in an optically accessible 2D flow channel. The appearance of cavitation depending on the pressure ratio p_{rail}/p_{out} is examined for different tapering. As seeding particles can serve as cavitation nuclei and therefore influence cavitation, the velocity measurements are conducted without particles.

2 Setup

To investigate erosion caused by cavitation under diesel-like conditions, a test bench was built up. It consists of a high pressure generator, which supplies the test section with calibration fluid ISO 4113 at a rail pressure up to 500 bar and temperatures between 25 °C and 120 °C. Pressure and temperature sensors are located upstream and downstream of the test section. The cavitation number σ (see equation 1) is set by adjusting a back pressure valve behind the test section.

$$\sigma = \sqrt{\frac{p_{rail} - p_{out}}{p_{rail}}} \tag{1}$$

For the present paper converging and diverging throttle geometries are used. They share the same inlet radius, throttle height and length. The dimensions of the diverging test section are shown in figure 1. The minimum height h is in the range of 100 to 300 µm, the length is 750 µm and the depth is 300 µm. It is made of stainless steel to prevent erosion during the measurements. These two flow channels are compared to a test section with parallel walls. Here the channel height differs. It is 300 µm (see Hosbach et al. (2018) for further details).
To capture the cavitation within the test section, an optical setup for shadowgraphy is applied (see figure 2).

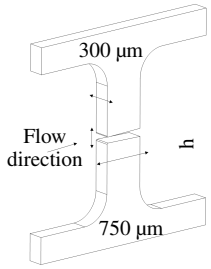

Figure 1: Diverging flow channel

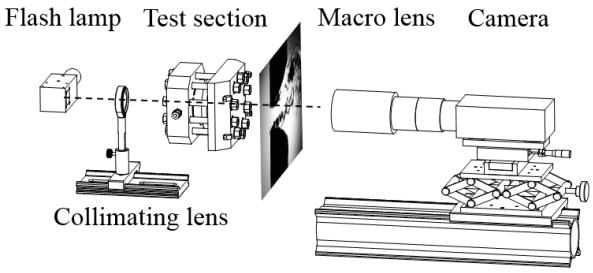

Figure 2: Optical setup

It consists of a 4 MP CMOS double frame camera, which enables to capture two frames of the flow with an interframe time of 180 ns, a flash lamp illuminating the cavitating flow for 39 ns and a macro lens. With this setup an enlargement scale of 0.85 µm/px is achieved.
The emitted light is deflected on its way from the light source to the camera sensor at the phase boundary between liquid and vapor due to a sudden density drop. Consequently cavitation structures appear dark, whereas liquid area is bright (see figure 3). The average gray scale value is calculated from a set of hundred frames to receive the average cavitation probability (see figure 4) and its corresponding standard deviation (see figure 5). Blue areas indicate high values for cavitation probability and standard deviation respectively whereas areas with a low cavitation probability and standard deviation respectively are painted red.

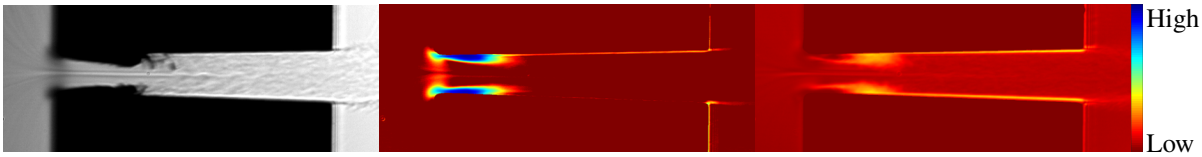

Figure 3: Raw image Figure 4: Cavitation probability Figure 5: Standard deviation

operating conditions: p_{rail} =100 bar, σ =0.70, T_{in} =40 °C

For the shadowgraphy PIV measurements the test section is illuminated by a double pulse Nd:YAG Gemini 200-15 laser. Its low pulse width of 3-5 ns enables sharp images. Due to the emission of coherent light, losses in image quality such as speckles have to be accepted. However, their effect can be reduced by image processing and by increasing the number of frames for averaging.

As seeding particles would strongly influence the cavitating inception and appearance, floating cavitation structures were used as pattern for the velocity evaluation instead.

3 Results: effect of back pressure on the cavitation length

Measurements, which will be presented below, reveal that back pressure has influence on cavitation length. λ is defined as the normalized cavitation length. It is measured by using the standard deviation of the calculated cavitation probability (see figure 4 and 5):

$$\lambda = \frac{cavitation\,length}{throttle\,length} \tag{2}$$

In figure 6, λ is plotted over the cavitation number σ for different geometries, i.e. the channel walls are either diverging, converging or parallel.

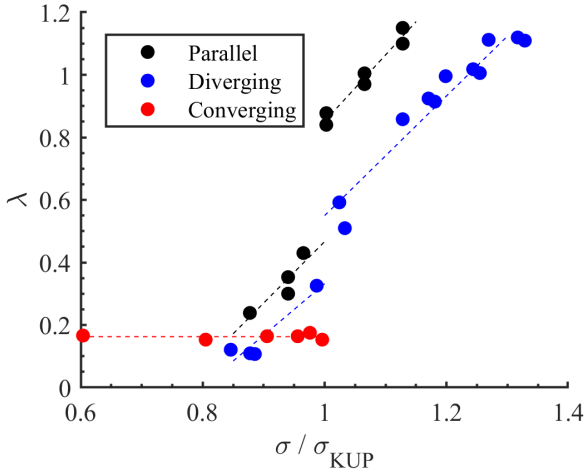

Figure 6: Normalized cavitation length vs. normalized cavitation number for different geometries

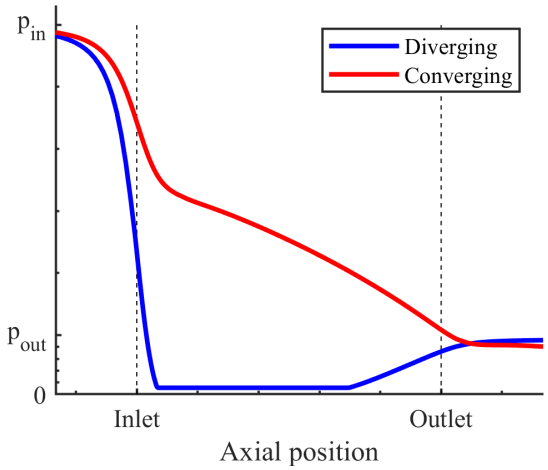

Figure 7: Schematic static pressure profile along the center line

σ_{KUP} is defined as the cavitation transition point at which the choked flow condition for the throttle is satisfied, i.e. a further reduction of the back pressure does not lead to an increase of mass flow, because the maximum flow speed is equal to the speed of sound of the liquid vapor mixture. The cavitation numbers at the cavitation transition point for the three flow channels apply to the relation: $\sigma_{KUP,div} < \sigma_{KUP,par} < \sigma_{KUP,conv}$.
It was found that for the converging flow channel, the cavitation length is almost constant for all cavitation numbers. This can be due to the fact that the overall static pressure level is higher in this case than in the diverging flow channel (see figure 7). Therefore no or only slight cavitation in the shear layer occurs. When further lowering the back pressure, the pressure level is still much higher than the vapor pressure of the liquid and consequently the low extent of the cavitation region is constant. The mass flow still increases when lowering the back pressure as the flow cross-section is not limited by cavitation.
In the case of a diverging flow channel, the pressure drop inside the throttle is higher. A comparatively big area is covered by cavitation structures which limits the flow cross-section. The cavitation length increases when lowering the back pressure. The cavitation transition point is reached for the lowest cavitation number $\sigma_{KUP,div}$ of all three flow channels.
The schematic static pressure profiles are derived from basic calculations using the Schnerr and Sauer cavitation model and a standard k-ε turbulence model.
A sudden increase in cavitation length is visible for $\sigma = \sigma_{KUP}$ in the diverging (compare figures 8 and 9) and the parallel flow channel.
The normalized cavitation length of the parallel flow channel is permanently higher than the cavitation length of the diverging throttle. This can be due to different channel heights. The parallel channel height is larger

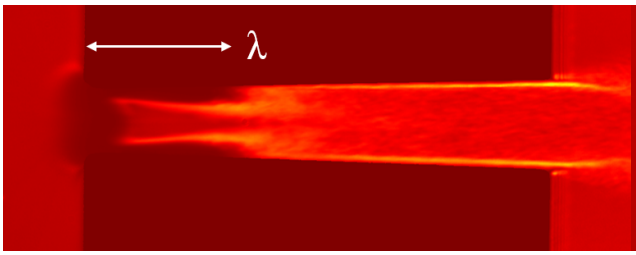

Figure 8: λ in the diverging flow channel for $p_{rail} = 500\,bar$, $\sigma/\sigma_{KUP} = 0.987$

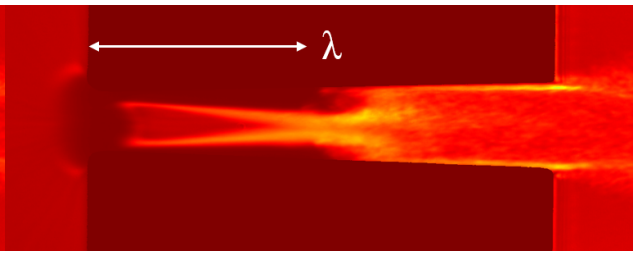

Figure 9: λ in the diverging flow channel for $p_{rail} = 500\,bar$, $\sigma/\sigma_{KUP} = 1.024$

than the diverging channel height. In Winklhofer et al. (2001) it was found that for the same throttle height the cavitation length in a parallel flow channel is slightly less to about the same as in a diverging flow channel. In the present case, varying the temperature in the range between 25 °C and 120 °C has no significant influence on the normalized cavitation length λ as a function of the normalized cavitation number σ/σ_{KUP}.

4 Results: effect of back pressure on the velocity field of a converging-diverging throttle

For a deeper understanding of the overall flow conditions, first basic velocity measurements in the diverging part of a converging-diverging flow channel (see figure 10) were carried out. The throttle is enlarged in comparison to the ones examined before so that velocity measurements are facilitated. This ensures traceable cavitation structures. In the convergent flow channel mentioned above, almost no cavitation is visible, so no velocity measurements are feasible.
A set of 2000 double frames with an interframe time of 250 ns are captured to calculate the average velocity (see figure 11). The movement of the cavitation structures can be correlated using PIV algorithms. The calculation is done in three cycles with a digressive interrogation window of $(96\text{ px})^2$ and $(48\text{ px})^2$.
Only areas where the phase boundary between cavitation and liquid is present, can be used for calculation. All other areas like pure liquid or pure cavitation do not show traceable structures and are therefore excluded from the calculation. Cavitation is a transient phenomenon, i.e. the cavitation length varies in time. So by using a big number of double frames to calculate the average velocity, it is more likely to cover a large area with traceable structures.

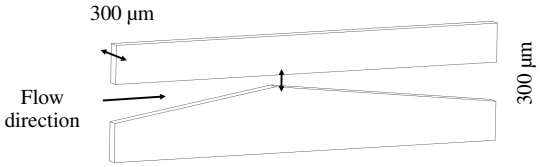

Figure 10: convergent-divergent flow channel

Figure 11: Raw image for PIV evaluation

It is important to mention, that with this evaluation approach the speed of the phase boundary and not the actual flow speed is measured.
For this series of measurements, the rail pressure p_{rail} =100 bar and the inlet temperature T_{in} =40 °C were held constant. In figure 12 the velocity field for a super cavitation regime and normalized cavitation number of $\sigma/\sigma_{KUP} = 1.19$ is shown. One can detect an increase of the streamwise velocity. A fast core jet is surrounded by a slower flow near the walls. At the axial positions x_1 and x_2, the velocity rises quickly in the shear layer from zero velocity at the wall to a rather uniform velocity (see figure 14). The center region of the flow is permanently free of cavitation. So no traceable structures and consequently no data are available here. Further downstream at the axial position x_2 (see figure 15) cavitation is more outspread. Lowering the back pressure results in a broader velocity plateau. This velocity lies in the range between 60 m/s and 70 m/s at the position x_2 comparing to the mean velocity derived from the measured mass flow $u_{\dot{m}}$ =95 m/s. It is assumed that the speed of the liquid flow is higher than the speed of the phase boundary to observe the conservation of mass. In Mauger et al. (2014) the calculated velocities are about 6 % less than the velocities derived from the measured mass flow. For super cavitation conditions the difference increases.

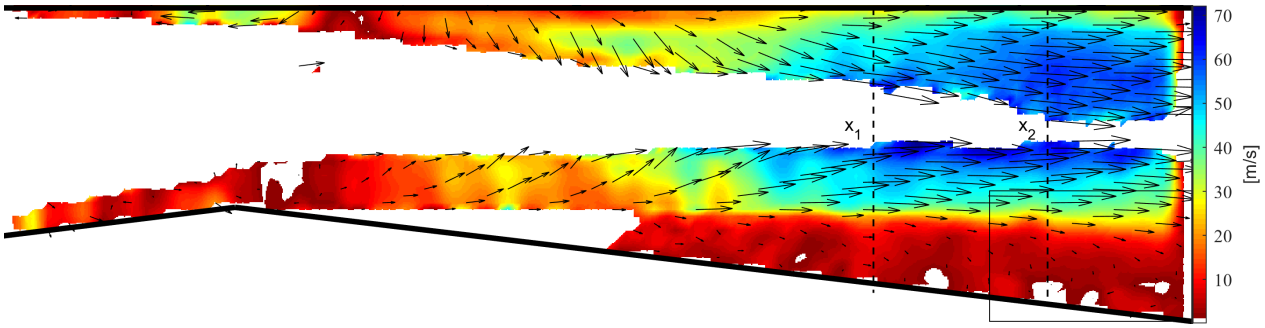

Figure 12: Velocity field for p_{rail} =100 bar, σ/σ_{KUP} =1.19, T_{in} =40 °C

In figure 13 the lower right part of figure 12 (black rectangular) is enlarged. Here rear-facing velocity vectors in the shear layer and the formation of eddies are visible at the tip of cavitation close to the channel wall where cloud detachment occurs. These observations confirm the findings of Schmidt et al. (2016).

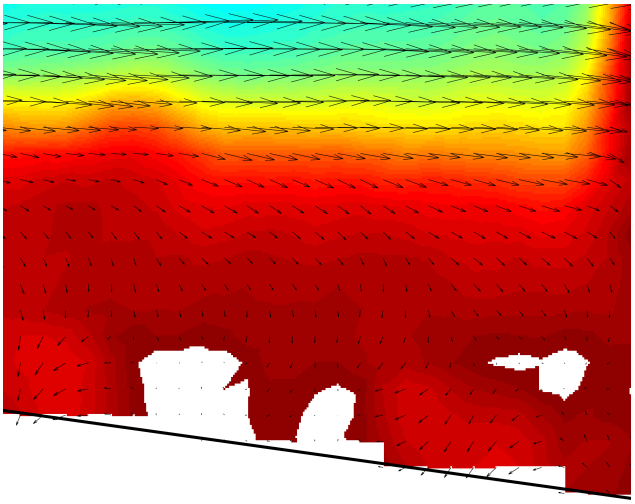

Figure 13: Eddy formation at the cavitation tip

The calculated Reynolds number in the visible flow section (compare figure 12) shows turbulent flow conditions: $9000 < Re < 11500$. The Reynolds number is defined as follows:

$$Re = \frac{\rho u_{\dot{m}} D_h}{\mu} \tag{3}$$

Here, ρ is the liquid density, $u_{\dot{m}}$ is the velocity derived from the measured mass flow, D_h is the hydraulic diameter and μ is the dynamic viscosity.
The overall uncertainty of the measured velocity field in figure 13 is about 5.4 %. It is defined as:

$$U_v = \sigma_v \sqrt{\frac{1}{N}} \tag{4}$$

with the standard deviation of the velocity σ_v and the number of velocity vectors per pixel N.

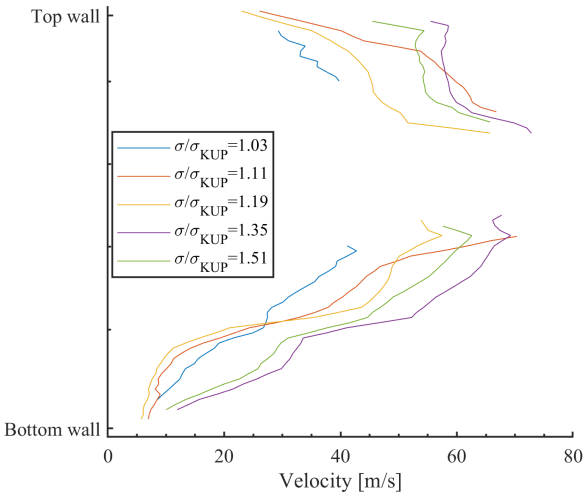

Figure 14: Velocity profiles at position x_1

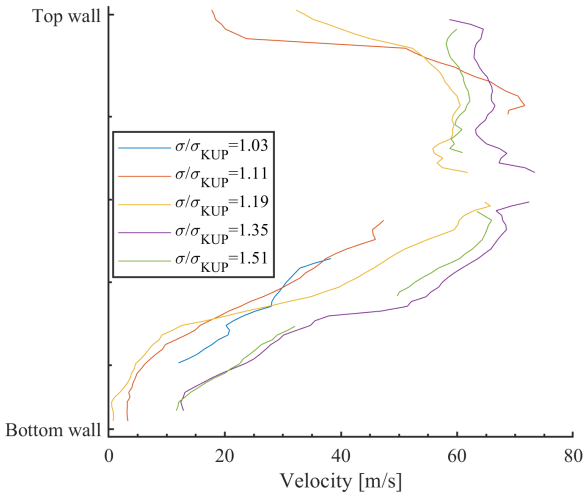

Figure 15: Velocity profiles at position x_2

5 Conclusion

An optically accessible 2D flow channel is used for a deeper insight into cavitation. Cavitation length as a function of taper and back pressure as well as the velocity in a converging-diverging flow channel are investigated. It was found that the cavitation length in the converging flow channel is constant when lowering the back pressure. It suddenly increases in the parallel and diverging throttle when reaching the cavitation transition point. Temperature has no significant influence on λ as a function of σ/σ_{KUP}.
For a deeper understanding of the overall flow conditions, first basic velocity measurements in a converging-diverging flow channel were carried out. It was found that the velocity of the phase boundary is lower than the velocity derived from the measured mass flow. A change in the shape of velocity profiles when lowering the back pressure was identified. A recirculation flow and eddy formation at the cavitation tip is visible.
For the future further measurements are planned to entirely understand the effect of geometric parameters like taper on cavitation in flow channels.

References

Hayashi, Shota and Keiichi Sato (2014). "Unsteady Behavior of Cavitating Waterjet in an Axisymmetric Convergent-Divergent Nozzle: High Speed Observation and Image Analysis Based on Frame Difference Method". In: *Journal of Flow Control, Measurement & Visualization* 02.03, pp. 94–104. DOI: 10.4236/jfcmv.2014.23011.

Hosbach, Markus, Tobias Sander, Uwe Leuteritz, and Michael Pfitzner (2018). "Temperature and pressure effects on cavitation erosion in diesel-like fuels". In: *10th International Symposium on Cavitation*.

Mauger, Cyril, Loïc Méès, Marc Michard, and M. Lance (2014). "Velocity measurements based on shadowgraph-like image correlations in a cavitating micro-channel flow". In: *International Journal of Multiphase Flow* 58, pp. 301–312. DOI: 10.1016/j.ijmultiphaseflow.2013.10.004.

Sato, Keiichi, Yuta Taguchi, and Shota Hayashi (2013). "High Speed Observation of Periodic Cavity Behavior in a Convergent-Divergent Nozzle for Cavitating Water Jet". In: *Journal of Flow Control, Measurement & Visualization* 01.03, pp. 102–107. DOI: 10.4236/jfcmv.2013.13013.

Schmidt, Aaron, B. Terry Beck, and Mohammad H. Hosni (2016). "Particle Image Velocimetry Measurements Near the Onset of Cavitation in a Converging-Diverging Glass Nozzle". In: *Volume 7: Fluids Engineering*. ASME, V007T09A044. DOI: 10.1115/IMECE2016-67384.

Sou, Akira, Shigeo Hosokawa, and Akio Tomiyama (2007). "Effects of cavitation in a nozzle on liquid jet atomization". In: *International Journal of Heat and Mass Transfer* 50.17-18, pp. 3575–3582. DOI: 10.1016/j.ijheatmasstransfer.2006.12.033.

Winklhofer, Ernst, Eberhard Kull, Erich Kelz, and Alexander Morozov (2001). *Comprehensive hydraulic and flow field documentation in model throttle experiments under cavitation conditions*. Zürich.